1988

The Effective Flow and Force Areas in Compressor Valves

C. J. Deschamps
Federal University of Santa Catarina

R. T. S. Ferreira
Federal University of Santa Catarina

A. T. Prata
Federal University of Santa Catarina

THE EFFECTIVE FLOW AND FORCE AREAS IN COMPRESSOR VALVES

C.J. Deschamps, R.T.S. Ferreira, A.T. Prata

Department of Mechanical Engineering
Federal University of Santa Catarina
88.049 - Florianópolis, SC - Brazil

ABSTRACT

This work presents the numerical results for dimensionless effective flow and force areas, different flow Reynolds numbers and valve separations, when the ratio of the valve to port diameter is varied from 1.5 to 5 and the exit port radius varies from 0.1 to 0.5. The flow Reynolds number covers the laminar regime and the dimensionless valve separation varies up to 0.04. Experimental results of the pressure distribution along the flapper valve are used for the validation of the numerical solution. A brief description of the experimental setup and the problem formulation used for the numerical solution are presented.

NOMENCLATURE

A_{ef}	dimensionless force area, equation (6)
A_{ep}	dimensionless flow area, equation (7)
D	valve disc diameter
d	orifice diameter
e	orifice length
F	dimensionless force acting on the valve disc
h	separation between valve disc and seat
k	isentropic coefficient (Cp/Cv)
$\dot{m}$	mass flow rate
P	dimensionless pressure, equation (4)
p	pressure
P_{atm}	atmospheric pressure
P_m	upstream pressure
ΔP_v	pressure drop across valve system
R	gas constant
R	dimensionless radial coordinate
r	radial coordinate
Re	Reynolds number, $Re = \rho \bar{u} d/\mu$
r_p	P_{atm}/P_m
r_s	exit port radius
T_m	upstream temperature
U,V	dimensionless velocity components in the x and r directions, equation (4)
u,v	velocity components in the x and r directions
$\bar{u}$	mean velocity through orifice
X	dimensionless axial coordinate
x	axial coordinate
μ	dynamic viscosity
ρ	density

INTRODUCTION

In order to determine the most important parameters for the performance analysis of valve systems of hermetic compressors, it is necessary a full understanding of the flow field of the gas flowing through the valves. This understanding is particularly important for the reed type valves because the flow is responsible for opening and closing those valves, which are said to be automatic.

The analysis of the flow field throughout automatic valves can become very complex and laborious, especially if the system geometry is fully taken into account. In order to get a good approximation of this type of flow, simpler geometries are used. The flow throughout radial diffusers can be considered the basic problem for performance analysis of valve systems, and is the geometry employed in the present investigation.

Many investigators have studied this problem in the past because it serves as a basis for numerous technological applications. Besides the significance of those results for hermetic compressors valves design, the analysis of air thrust bearings and aerosol impactors are additional examples.

A good review of the theoretical and experimental works published before 1956 is presented by Woolard [1]. A paper by Ferreira and Driessen [2] presents a discussion of different types of flow found in reed type valves and an updated bibliographic review.

The numerical solution, experimentally validated, of the laminar, incompressible flow field of air in radial diffusers, for small separation between discs has been recently presented [3,4].

Different valve, port and seat geometries affect the effective flow area and the effective force area. Those parameters are needed for the numerical simulation of hermetic compressors and they can also be used to evaluate the expected performance of a compressor valve.

This paper presents the results of dimensionless effective flow and force areas for different magnitudes of the exit port radius and different valve diameters, for various flow Reynolds numbers and valve separations. Those results are calculated for laminar incompressible flow and for small distances between valve and seat.

PROBLEM FORMULATION

The flow region of importance is shown in Fig. 1. The flow is axially symmetric: thus only half of the diffuser is shown. As shown in the figure, the gas is fed through an orifice of diameter d, length e and port exit radius r_s. The same flow geometry is found in reed type valves of hermetic compressors in which the orifice is the valve port located in the valves plate, and the upper disc is the reed.

Through the feeding orifice the flow is initially in the axial direction (x-direction) and close to the reed it is deflected to the radial direction (r-direction). As indicated in Fig. 1 the valve disc diameter is D and the separation between the valve disc and the seat is h.

The flow is considered to be laminar, incompressible, and isothermal, and it is governed by continuity and Navier-Stokes equations. In dimensionless form, these equations can be written as

$$\frac{\partial}{\partial X}(RU) + \frac{\partial}{\partial R}(RV) = 0 \tag{1}$$

$$U\frac{\partial U}{\partial X} + V\frac{\partial U}{\partial R} = -\frac{\partial P}{\partial X} + \frac{1}{R}\frac{\partial}{\partial R}\left(R\frac{\partial U}{\partial R}\right) + \frac{\partial^2 U}{\partial X^2} \tag{2}$$

$$U\frac{\partial V}{\partial X} + V\frac{\partial V}{\partial R} = -\frac{\partial P}{\partial R} + \frac{1}{R}\frac{\partial}{\partial R}\left(R\frac{\partial V}{\partial R}\right) + \frac{\partial^2 V}{\partial X^2} - \frac{V}{R^2} \tag{3}$$

where U and V are dimensionless axial and radial velocity components, respectively, and P is the dimensionless pressure. In Eqs.(1)-(3) the non-dimensional quantities are defined as follows:

$$X = x/d \quad , \quad R = r/d$$

$$U = \rho u d/\mu \quad , \quad V = \rho v d/\mu \quad , \quad P = \rho p/(\mu/d)^2 \tag{4}$$

where ρ and μ are the fluid density and the fluid absolute viscosity, respectively.

Eqs.(1)-(3) are subject to the following boundary conditions: (i) solid walls, U=V=0; (ii) along the symmetry axis (R=0), V=∂U/∂R=0; (iii) at the orifice entrance two different boundary conditions have been used, U=Re (uniform flow) and $U=2Re(1-4R^2)$ (Poiseuille flow), where $Re=\rho\bar{u}d/\mu$ is the flow Reynolds number defined in terms of the mean velocity through the orifice of diameter d; (iv) at the diffuser exit, U=∂(VR)/∂R=0. In the discussion of the results, the validity of those boundary

conditions has been checked.

At this point the formulation of the problem has been completed. As one can see the only non-geometric parameter to be prescribed is the flow Reynolds number. Next, the methodology adopted in the solution will be presented.

NUMERICAL METHOD

The differential equations governing the laminar flow field and the associated boundary conditions were solved using the finite volume method [5] . In this method the solution domain is divided into non-overlapping control volumes. The differential equations are integrated over each one of the control volumes generating a set of algebraic equations. The velocity and pressure fields are obtained from the simultaneous solution of these algebraic equations. The SIMPLER algorithm of Patankar [6] has been used for the numerical solution of the algebraic equations. This method of solution has been used routinely to solve fluid flows problems. To accelerate the convergence of the solution the block correction algorithm [7] has been introduced into the computer program.

Especial attention has to be devoted to the mesh selection for the integration of the differential equations because the flow field shows very high velocity gradients and the false diffusion in the numerical method and the computer time have to be minimized.

In the presence of steep velocity gradients, which happen at the exit of the feeding orifice, the number of nodal points had to be increased sufficiently.

The false diffusion is one of the inconvenients of the numerical methods. If the local velocity vector is not aligned with one of the coordinate axis and the velocity module is sufficiently high, physically inexisting contributions of the variables are introduced into the equations generating errors in the solution. In order to reduce the false diffusion, a mesh refinement is introduced. Further details about false diffusion can be found in [8].

In the process of mesh refinement, the solution of the flow field was monitored for each new mesh. There was a compromise between the improvement in the solution and the computer time necessary for its convergence. Further details with respect to the process of mesh refinement can be found in [9].

EXPERIMENTAL SETUP AND PROCEDURES

Fig. 2 presents a schematic general view of the experimental setup. Compressed air stored in two tanks with approximately 1 m^3 and maximum pressure of 11 bar flowed through a 75 mm x 6.5 m (diameter x length) pipe before getting to the test section. The pipe is kept leveled by means of six equally spaced supports. A flowrate control valve and a calibrated orifice flow meter are mounted in the pipeline. The relations used in the experiment for the valve disc and the feeding orifice are D/d=3 and e/d=0.933 where d=30 mm.

A small chamfer ($\ell \leq 0.38$ mm) has been detected at the exit port section in the experimental model. Therefore this bevel has been considered in the validation process of the numerical scheme.

Fig. 3 shows the valve seat, the diffuser feeding orifice, the valve reed and the positioning system used in setting up the frontal disc.

The pressure distribution along the valve disc is used for the validation of the numerical solution therefore the frontal disc has a especial feature, as shown in Fig. 4. Along the reed diameter there is a sliding bar provided with a small tap hole (0.7 mm diameter) and an internal connecting perforation up to one of the ends of the bar and then connected to a differential pressure inductive transducer. At the other end of the sliding bar an inductive displacement transducer is attached in order to supply the instantaneous position of the tap hole. Both signals from the inductive transducers are introduced in an amplifier bridge and after to an on-line x-y plotter. As soon as the sliding bar is moved along the diameter of the valve disc, the x-y plotter draws the pressure distribution simultaneously. The maximum rating of the differential pressure transducer is 0.01 bar and the displacement transducer is ± 100 mm.

A positioning system was used to furnish the right position for the valve disc and this constitutes an important feature in this experiment. Both discs have to be concentric, parallel and placed at a certain distance one from the other. A micrometric table was used to measure the distance between the valve disc and the seat.

After getting the final positioning of the discs the data is taken. The main quantities measured in each experimental run are: pressure distribution along the valve disc, mass flowrate in the diffuser and the distance between the valve disc and the seat. The mass flow rate through the diffuser was obtained via the pressure drop across a calibrated orifice plate flowmeter with a minimum diameter of 15 mm. This pressure drop was measured by an inductive differential pressure transducer with maximum rating of 0.01 bar.

The uncertainty analysis associated to the experimental results was performed following Moffat's methodology |10|. The maximum experimental uncertainty, applicable to the pressure in the stagnation region of the valve disc, is less than 3%, for the valve separation the uncertainty is less than 1.5% and for the Reynolds number it is less than 1.1%. Additional information regarding the experimental setup and procedures are available in |9,11|.

RESULTS

Figs. 5 and 6 compare typical measured and numerically calculated pressure distribution on the circular valve reed. These Figs. considere the presence of a small bevel at the exit port section of the experimental model. The abcissa of Figs. 5 and 6 is the dimensionless radial position and the ordinate is the gauge pressure along the valve disc, $(p/(\rho\bar{u}^2/2))$. It is worth noting that $p/\rho\bar{u}^2 = P/Re^2$, where P is the dimensionless pressure as defined in Eq.(4). In Fig. 5 the flow Reynolds number is 695 and h/d = 0.0089, while in Fig. 6 Re = 1500 and h/d = 0.02177. The small values of h require a very careful setup preparation procedure. The experimental uncertainties associated to the measured values are indicated in Figs. 5 and 6.

The good agreement between experimental and numerical results, as shown in Figs. 5 and 6 lends evidence to the validity of the numerical solution.

The numerical results presented in this work are the dimensionless axial force acting on the valve disc and the dimensionless effective flow and force areas. The integration of the pressure distribution along the valve disc gives the axial thrust acting on the diffuser. In dimensionless form this force is given by

$$F = \int_0^{(D/2)/d} (2P/Re^2)\ 2\pi R\ dR \qquad (5)$$

The evaluation of the flow and force areas was performed using the same methodology described by Ferreira and Driessen |2|. In dimensionless form, using the port diameter d as a characteristic parameter, one gets

$$A_{ef} = F/\Delta P_v \qquad (6)$$

$$A_{ep} = \frac{\dot{m}/(d^2 p_m)}{\sqrt{\frac{2k}{(k-1)RT_m}}\sqrt{r_p^{2/k} - r_p^{(k+1)/k}}} \qquad (7)$$

Next the numerical results for the force F and the effective areas A_{ef} and A_{ep} are presented in order to analyze the influence of two different geometric parameters r_s/d and D/d. Three different valve separations were investigated h/d = 0.01, 0.02 and 0.04. For the r_s/d influence the relation D/d = 3 was used when the Reynolds number was varied, Re = 500, 900 and 1800. For the D/d influence the relation r_s/d=0 was used for the same Reynolds numbers indicated above. The results for Re=900 are not included.

Figs. 7, 8 and 9 present the r_s/d influence on the axial force F and on the effective force and flow areas A_{ef} and A_{ep}, respectively. Dashed lines are for Re=500

and continuous lines for Re=1800. For the small values of h/d and Re, as shown in Fig. 7, the force F decreases as r_s/d increases because the stagnation pressure in the central region of the disc also diminishes. However, for certain combinations of Re and h/d (higher values) F increases with r_s/d. For those valve separations and flow rates the exit port radius tends to reduce the recirculating region in the flow field which is responsible for the presence of the negative pressure region on the valve disc.

Fig. 8 shows that the effective flow area values increase as r_s/d increase for all investigated values of valve separations and flowrates. For the effective flow areas, as shown in Fig. 9 there is a moderate increase for the smaller values of Re and h/d. This is due to the reduction of the head loss when r_s/d increases. For the higher values of Re and h/d there is an additional increase on A_{ep} , as r_s/d increases, because the recirculating region in the diffuser also decreases.

Figs. 10, 11 and 12 show the D/d influence on the axial force F and on the effective force and flow areas A_{ef} and A_{ep} , respectively. Dashed lines are for Re=500 and continuous lines for Re=1800.

For Re=500, there is a continuous growth of the force F as D/d increases, as shown in Fig. 10. This is due to the increase in the pressure values in the stagnation region and also due to the higher values of the actuating pressure areas. As the diffuser length increases the pressure distribution along the valve disc reaches higher values. This is also responsible for the reduction of A_{ep}, for Re=500, shown in Fig. 12.

For Re=1800 and h/d=0.04, as shown in Fig. 12, the effective flow area for D/d=1.5 is smaller than for D/d=2.0. Possibly the separation region for this situation is longer than the diffuser length and the flow is unable to reattach inside the diffuser. Moreover the growth of the separation bubble produces the reduction of the diffuser area available for the flow. This leads to a reduction in A_{ep} and produces a higher stagnation pressure in the central region of the valve disc with higher values for F, Fig. 10 and A_{ef} , Fig. 11.

CONCLUSIONS

The present work presents the numerical results of the laminar, incompressible, isothermal flow in radial diffusers for small separations between discs in order to determine the influence of the exit port radius and the valve diameter on the effective flow and force areas. Experimental results have been used for the validation of the numerical model. The motivation for this type of flow comes from the importance of these parameters for the compressor valves design. Curves for the axial force on the valve disc and for the effective flow and force areas are presented for different flow rates and discs separations.

ACKNOWLEDGEMENTS

The authors acknowledge the permission to publish this paper by Empresa Brasileira de Compressores S/A - EMBRACO. This research is part of a technical-scientific agreement between Federal University of Santa Catarina and EMBRACO.

REFERENCES

[1] Woollard, H.W., A Theoretical Analysis of the Viscous Flow in a Narrowly Spaced Radial Diffuser, J. Appl. Mech. - Trans. ASME, 24, 9-15, 1957

[2] Ferreira, R.T.S., and Driessen, J.L., Analysis of the Influence of Valve Geometric Parameters on the Effective Flow and Force Areas, 8th Purdue Compressors Technology Conference, West Lafayette, Indiana, pp.632-646, Aug.1986.

[3] Prata, A.T., Ferreira, R.T.S., and Deschamps, C.J., Laminar Flow in Radial Diffusers - Computation and Experiment, 1st National Meeting of Thermal Sciences, Rio de Janeiro, pp. 63-66, 1986 (in Portuguese).

[4] Ferreira, R.T.S., Prata, A.T., and Deschamps, C.J., Laminar Fluid Flow in Compressor Valves - Numerical and Experimental Results, Fluid Flow and Heat Transfer in Reciprocating Machinery, Winter Annual Meeting, Boston, pp.33-38, 1987.

[5] Patankar, S.V., Numerical Heat Transfer and Fluid Flow, Hemisphere, Washington, 1980.

[6] Patankar, S.V., A Calculation Procedure for Two-Dimensional Elliptic Situations, Numerical Heat Transfer, 4, 409-425, 1981.

[7] Settari, A., and Aziz, K., A Generalization of the Additive-Correction Methods for the Iterative Solution of Matrix Equation, SIAM J. Numerical Analysis, 10 506-521, 1973.

[8] Raithby, G.D., A Critical Evaluation of Upstream Differencing Applied to Problems Envolving Fluid Flow, Computer Methods in Appl. Mech. Engng, 9, 75-103, 1976.

[9] Deschamps, C.J., Laminar Fluid Flow Through Compressor Valves, M.Sc. Thesis, Department of Mechanical Engineering, Federal University of Santa Catarina, Florianópolis, Brazil, 1987 (in Portuguese)

[10] Moffat, R.J., Contributions to the Theory of Single-Sample Uncertainty Analysis, J. Fluids Engng. - Trans. ASME, 104, 250-260, 1982.

[11] Ferreira, R.T.S., Deschamps, C.J., Prata, A.T., Pressure Distribution Along Valve Reeds of Hermetic Compressors, 1st Int. Conf. on Experimental Heat Transfer, Fluid Mechanics and Thermodynamics, Yugoslavia, 1988.

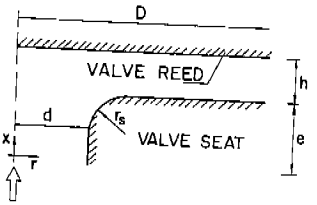

Fig. 1 - Flow geometry

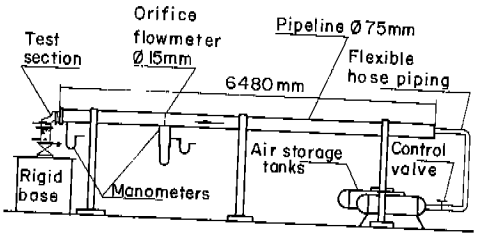

Fig. 2 - Schematic general view of experimental setup

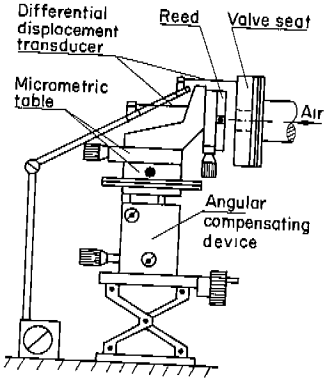

Fig. 3 - Test section and positioning system

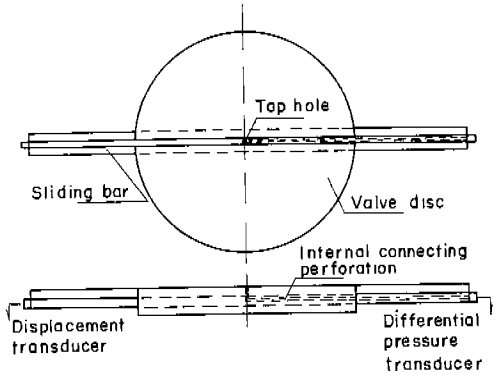

Fig. 4 - Valve reed with sliding tap hole

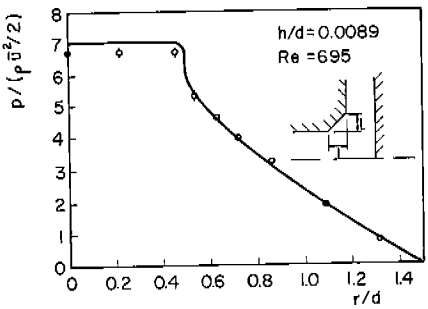

Fig. 5 - Comparison of numerical and experimental results for h/d=0.00890 and Re=695

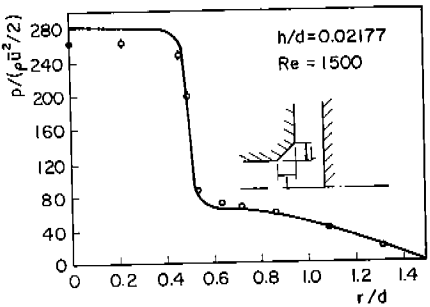

Fig. 6 - Comparison of numerical and experimental results for h/d=0.02177 and Re=1500

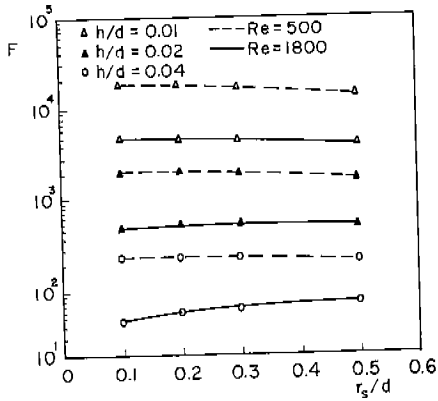

Fig. 7 - Influence of exit port radius on the force acting on the disc

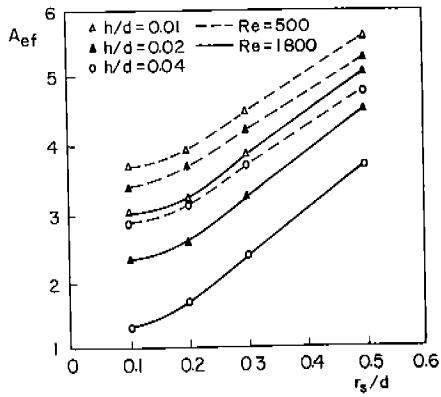

Fig. 8 - Influence of exit port radius on the effective force area

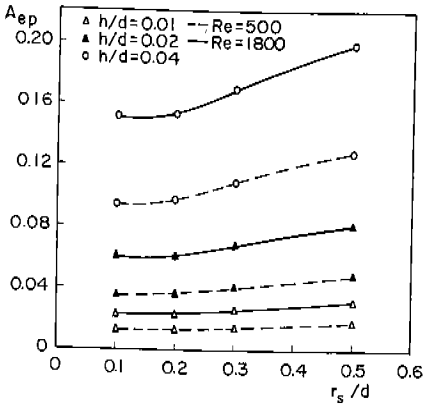

Fig. 9 - Influence of exit port radius on the effective flow area

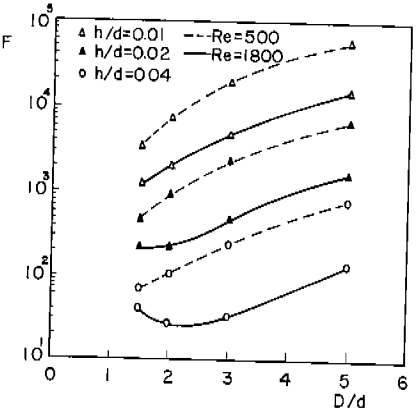

Fig. 10 - Influence of valve plate diameter on the force acting on the disc

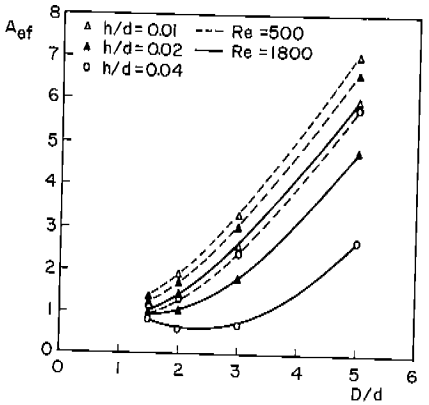

Fig. 11 - Influence of valve plate diameter on the effective force area

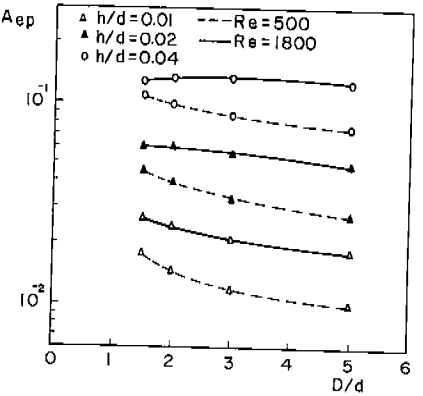

Fig. 12 - Influence of valve plate diameter on the effective flow area